EXTRACTION OF WIND EROSION OBSTACLES BY INTEGRATING GIS-DATA AND STEREO IMAGES

Y. J. Zhang [a, b]

[a] School of Remote Sensing and Information Engineering, Wuhan University, Wuhan, Hubei, 430079, P.R. China
[b] Supresoft Inc, 3-2#Building, Guandong Science Park, 2nd Guanshan Road, Wuhan, Hubei, 430074, P.R. China

yjzhang@supresoft.com.cn

Theme Session 12

KEY WORDS: Extraction, Integration, GIS, Image, Analysis, Vegetation, Classification

ABSTRACT:

Data integration is a very important strategy to obtain optimum solutions in geo-scientific analysis, 3D scene modelling and visualization. This paper mainly focuses on the integration of GIS-data, stereo aerial imagery and DSM to derive automatically wind erosion obstacles in the open landscape to enhance the Digital Soil Science Map of Lower Saxony in Germany. The extracted wind erosion obstacles can be used to derive wind erosion risk fields for soil monitoring and preservation. GIS-data is used as prior information for the object extraction. The GIS-objects roads, field boundaries, rivers and railways from GIS database can represent initial search areas for extracting wind erosion obstacles, which are often located parallel and near to them. Wind erosion obstacles are divided in the semantic model into hedges and tree rows, because of different available information from the GIS-data, although their extraction strategies are similar. Different approaches, such as segmentation by NDVI and CIE L*a*b, edge extraction, linking, grouping and verifying with 3D information, are combined to extract the objects of interest. The extracted wind erosion obstacles are integrated into a semantic model, described by their 3D appearance in geometry, together with 2D elongated shadow regions in a known direction according to 3D information and sunshine.

1. INTRODUCTION

In geo-scientific analysis, estimation of potential erosion areas, soil monitoring and preservation, the integration of different data sources is an important strategy to obtain overall solutions. To facilitate automated object extraction from aerial imagery, the use of prior knowledge is essential (Baltsavias 2002, Straub 2003). This paper mainly focuses on extraction of wind erosion obstacles by data integration to enhance the Digital Soil Science Map of Lower Saxony (Germany) in the open landscape. GIS-data, aerial stereo imagery and digital surface models (DSM) are used as sources of information. The extracted wind erosion obstacles can be used to derive potential wind erosion risk fields together with information of prevailing wind direction, field width and soil parameters.

Digital color infrared (CIR) imagery is an important development in data acquisition and update especially for vegetations (Englisch and Heipke 1998). The Normalized Difference Vegetation Index (NDVI) is widely used in photogrammetry and remote sensing applications, such as monitoring of vegetation condition and production in different environmental situations (Prince 1991), change detection (Lyon et al 1998), extracting of trees in urban areas (Straub 2003) and detecting smoke effects of vegetations (De Moura 2003). The CIE L*a*b color space is mainly used in computer vision communities for image analysis and industrial applications (Pierce 1994, Campadelli 2000, Lebrun 2000). Nevertheless, it seems not of much interest by photogrammetrists despite its powerfulness in image classification and analysis.

Although considerable results have been achieved, the extraction of vegetation objects from high-resolution imagery is still not in an advanced period (c.f. Heipke et al. 2000, Straub 2003). Prior work of extraction of wind erosion obstacles in the open landscape is much more marginal. Our specific task is to extract wind erosion obstacles to enhance the soil map for potential utilization of soil monitoring and preservation. The related work of the specific task, such as semantic modeling, extraction and updating of field boundaries (Butenuth 2003) are not of interest in this paper, although wind erosion obstacles are often field boundaries or at least can help to extract field boundaries.

General strategy and the data sources used for extraction of wind erosion obstacles are described in the next section. Afterwards, the detailed approach for extraction of wind erosion obstacles, including image segmentation with NDVI and CIE L*a*b, line extraction and grouping, verifying with 3D information will be presented. Experimental results of automatically derived wind erosion obstacles in the open landscape are given in section 4 to demonstrate the potential of the proposed approach. Finally, conclusions are given and further work is highlighted.

2. GENERAL STRATEGY AND DATA SOURCES

2.1 General strategy

The enhance of Digital Soil Science Map with extracted wind erosion obstacles by integrating GIS-data, CIR stereo imagery as well as DSM are the content of the current work. GIS-data represents an initial scene description of the open landscape of interest. The object wind erosion obstacle is divided in hedge and tree row, because there are different information available from GIS data, although their extraction strategies are similar. The

non-vegetation areas in CIR images are removed by NDVI and CIE L*a*b. Afterwards, edges of tree rows and hedges are extracted with Canny edge extraction algorithm followed by line linking, grouping and matching. Lines belong to non-interested regions such as urban, forests in the stereo imagery are masked out by GIS-data. DSM is also integrated into line grouping approach because of usually short distance and low contrast in NDVI and CIE L*a*b information of pixels between hedge and tree row. Then the matched lines are projected onto the landscape with known camera parameters. 3D information provided by DSM is used to verify the potential wind erosion obstacles since they are always higher than the landscape. Finally, the objects of interest, wind erosion obstacles, are described by their characteristics and appearance in an overall context with other neighboring and influencing objects.

2.2 Data sources

The GIS data with accuracy of about 3 m consists of scene description of the German ATKIS DLMBasis (Authoritative Topographic Cartographic Information System, basic digital landscape model) (Butenuth 2003). Since only wind erosion obstacles are of interest, regions where no wind erosion obstacles exist (e.g. urban, water, forest) in the imagery can be masked out by the available GIS-data. Furthermore, the GIS-objects road, river and railway represent the approximate geometric position of parts of the field boundaries. They also represent potential search areas for wind erosion obstacles, which are usually located parallel and near to them. Figure 1 shows the GIS data superimposed on the aerial image in the open landscape. Roads and field boundaries are depicted in yellow, buildings in white and forests in green. A representative region of interest is represented in dashed white lines, separately shown in figure 2.

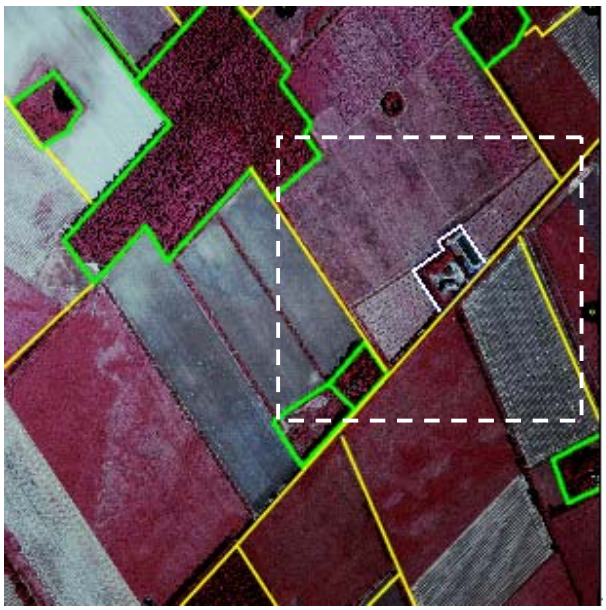

Fig. 1. Open landscape with superimposed GIS data

CIR images (with ground resolution of 0.5m in this paper) are generated in early autumn when the vegetation is in an advanced period of growth. The color is almost fully green for wind erosion obstacles, while for example light yellow for crops. This information is advantageous for automatic vegetation extraction. Therefore, the color space RGB, which presents the raw stereo CIR images, is transformed into a device type independent color space CIE L*a*b since it is powerful in image segmentation. The CIR aerial image is classified into vegetation and non-vegetation regions. Furthermore, classifying with NDVI is also possible. The two approaches are both used to segment the images into vegetation and non-vegetation areas. Of course, there are other objects than wind erosion obstacles, which will appear in green color such as grassland. That means GIS-data and CIR imagery are not enough to extract wind erosion obstacles.

Fig.2 Selected region of interest

Fig. 3. DSM superimposed with orthoimage

Additionally, corresponding DSM with 0.5 m ground resolution of the interested open landscape is obtained with VirtuoZo, which is developed by Supresoft Inc. The DSM is not precise because

control points are obtained from the 3m resolution GIS-data. The field of interest in the open landscape is mostly flat, and wind erosion obstacles are always higher. Thus, 3D information as shown in figure 3 is also one of the most useful sources of information, which can be integrated into a combined model together with GIS-data and color information to support the extraction of wind erosion obstacles.

3. EXTRACTION OF WIND EROSION OBSTACLES

3.1 Image segmentation

Image segmentation by NDVI value for CIR images to extract vegetations is a well-known approach (c.f. Lyon 1998, Butenuth 2003). NDVI calculations are based on the principle that actively growing green plants strongly absorb radiation in the visible region of the spectrum such as Red region while strongly reflecting radiation in the Near Infrared region and thus a high NDVI value (NDVI = (NIR-Red)/(NIR+Red)). There are other segmentation approaches based on Vegetation Index. They all give the similar results (Lyon 1998). So NDVI is used to segment the images in this paper. Sometimes, results of segmentation with NDVI are not very satisfying due to noises. The results have to be improved with other approaches.

In 1931, Commission Internationale de l'Eclairage (CIE) presented a device independent color space CIE XYZ, as shown in figure 4 (SEII EM-MI 2002). Generally, the points of surface $X+Y+Z=1$ are considered in the three-dimensional area. This surface includes the white point (Wx, Wy, Wz) with value $(0.312779,\ 0.329184,\ 0.358037)$ and three settlements for the basic colors R, G, B. Each point in color space RGB has its corresponding point in color space CIE XYZ.

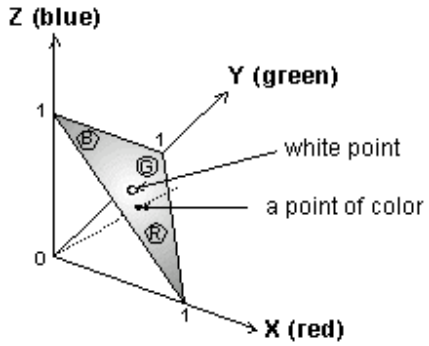

Fig. 4. Definition of CIE XYZ

We will simply give the transformation from RGB to CIE XYZ, please see (SEII EM-MI 2002) for more detail of how to derive the transformation model.

$$\begin{bmatrix} X \\ Y \\ Z \end{bmatrix} = \begin{bmatrix} 0.412291 & 0.357664 & 0.180209 \\ 0.212588 & 0.715329 & 0.072084 \\ 0.019326 & 0.119221 & 0.949102 \end{bmatrix} \bullet \begin{bmatrix} R \\ G \\ B \end{bmatrix} \quad (1)$$

The color space CIE L*a*b is announced in 1976 (SEII EM-MI 2002). The model CIE L*a*b refers a little to the models of colors expressed by the Newton's circle, as shown in figure 5.

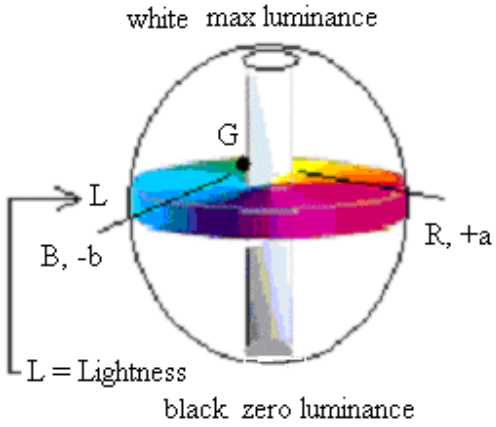

Fig. 5. Definition of CIE L*a*b

The component L represents the light Lightness with value from 0 to 100 as defined below.

$$\begin{aligned} L &= 116 \cdot (Y/Wy)^{1/3} - 16 \quad \text{if } 0.008856 < (Y/Wy) \\ L &= 903.3 \cdot (Y/Wy) \quad \text{else} \end{aligned} \quad (2)$$

The components a and b represent two differences defined below. In theory, component a varies from blue (with value –120) to red (with value +120), component b varies from green (with value –120) to yellow (with value +120).

$$\begin{aligned} a &= 500 \cdot (F(X/Wx) - F(Y/Wy)) \\ b &= 200 \cdot (F(Y/Wy) - F(Z/Wz)) \end{aligned} \quad (3)$$

Where (X, Y, Z) is the point to be converted, (Wx, Wy, Wz) the white point as the definition of CIE XYZ. The point (X, Y, Z) can be obtained from equation (1) with RGB value of a certain pixel in the image. $F(p) = p^{1/3}$ if $p > 0.008856$, otherwise $F(p) = 7.787 * p^{1/3} + 16/116$.

There is no direct relation between RGB and CIE L*a*b. The transformation from RGB to CIE L*a*b must be made indirectly through CIE XYZ. Firstly, RGB is transformed into CIE XYZ with equation (1), and then the received points into CIE L*a*b according to equation (2) and equation (3).

The component a of CIE L*a*b will be always positive for vegetations in the CIR imagery, and close to +120 for the strongest vegetative growth. So this information can be combined with NDVI to segment the CIR images. Figure 6 shows the segmented CIR image by NDVI and CIE L*a*b information. In order to keep all potential wind erosion obstacles, we adopt a relatively low threshold during segmenting. White areas in the

image are non-vegetation ones. When compared with figure 2, it can be seen that most non-vegetation regions are removed.

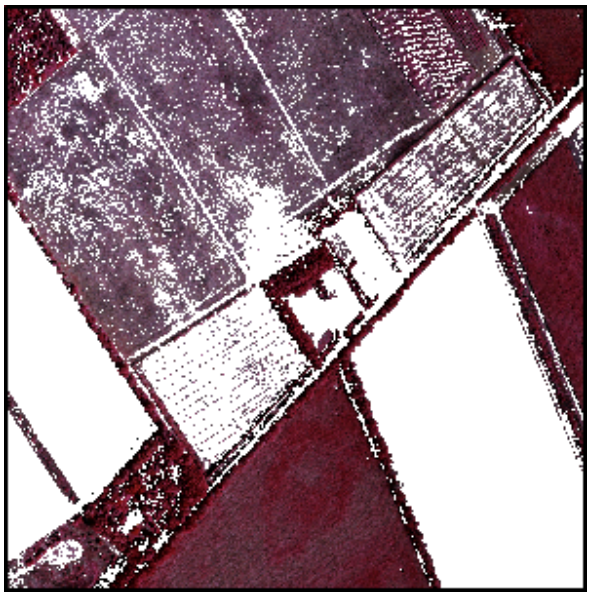

Fig. 6. Segmented CIR image

3.2 Line extraction and linking

Single tree and hedge are not of interest since they are nearly of no influence on soil science map. Wind erosion obstacles, no matter tree rows or hedges, usually appear line structures, or at least can be treated as combination of line segments. As can be seen from figure 6, wind erosion obstacles in the segmented image appear very good line structures. Canny edge extraction algorithm is used to extract these edges. Then the extracted edges are converted into line segments longer than a given length.

Fig. 7. Extracted image lines

As shown in figure 7, most wind erosion obstacles have their corresponding borderline segments. Lines of non-interested regions such as forests can be masked out with available GIS-data, for example the center part of figure 7. Field boundaries also appear line structures, as shown on the top of figure 7. These edges can be easily removed by post processing according to NDVI and CIE L*a*b information. But boundaries of grassland are difficult to remove because they also appear good line structure, high NDVI value and positive a component of CIE L*a*b, for example the right side of figure 7. Another reason is that wind erosion obstacles are sometimes connected to grassland (bottom-right of figure 7). They have to be treated as potential wind erosion obstacles at this step. Small line segments of potential wind erosion obstacles are linked along-line-direction based on their inclination, direction and distances in between by perceptual grouping techniques. The linked lines will be usually longer than the initial ones and represent the borderline of wind erosion obstacles (Figure 8).

Fig. 8. Linked line segments

3.3 Line grouping and matching

Tree rows and hedges always have two borders since they have a certain width. So the extracted lines of two borders (sometimes only borderline of one side can be extracted if the other side is connected to grassland or of low contrast in the image) should be grouped into one line segment. Corresponding line of the interested one of the same wind erosion obstacle can be determined by a search algorithm within a certain distance of the cross-line-direction. DSM information is also considered during line grouping. The line pairs are combined together to get the centreline of wind erosion obstacles. In Figure 9, all line pairs are successfully combined together.

If no corresponding line found, the line of interest will probably be the boundary of grassland and of course that of wind erosion obstacles. For boundary of grassland, one side of it will be a region with low NDVI value while the other side a homogeneous region with high NDVI value. This information is also helpful to

remove borderlines of grassland. Furthermore, centerlines of wind erosion obstacles can be obtained by least squares image matching with roof-template (Zhang et al. 2003).

Fig. 9. Grouped potential wind erosion obstacles

3.4 Verifying with 3D information

After image segmentation, line extraction and grouping on both images of one stereo, the matched lines are the centerlines of wind erosion obstacles. The conjugate lines on both images can be found with epipolar line and mean x-parallel of relative orientation because there are only a few candidates of conjugate of the interested line. A global optimization is needed to make sure that no false corresponding exists.

Fig. 10. Results of extracted wind erosion obstacles

The conjugate line pairs can be used to obtain the 3D lines in object space with known internal and external orientation parameters. Lines without conjugate on the other image can be initially projected onto a level plane with mean height of wind erosion obstacles. The new height value can be obtained from DSM with the projected plane coordinates. Then the image line can be projected onto a level plane with the new height. This recursive search procedure usually converges within a few iterations.

The obtained 3D lines are potential wind erosion obstacles. Roads, field boundaries, rivers and railways in GIS data are also potential search areas of wind erosion obstacles. All these information are compared with DSM to verify whether they are really wind erosion obstacles. At this point, the remained boundaries of grassland can be easily removed because grassland will be usually wider than wind erosion obstacles and thus a large area with same height information. Figure 10 shows the finally extracted wind erosion obstacles.

4. EXPERIMENTS AND RESULTS

In this section, experimental results of the proposed approach are presented. GIS data from ATKIS, stereo CIR imagery with known camera orientations, and DSM are used as sources of information. The general procedure of the proposed approach can be summarized as follows. Firstly, CIR image is classified into vegetation and non-vegetation areas, and non-vegetation areas are removed from the image. Afterwards, lines are extracted from the segmented image, followed by removing of extracted lines that belong to non-interested regions such as forests and buildings according to the available GIS-data. Then the remained lines are linked along-line-direction and then grouped cross-line-direction to get the centerline of wind erosion obstacles. Finally, camera parameters, matched lines, DSM and GIS data are integrated to derive true wind erosion obstacles.

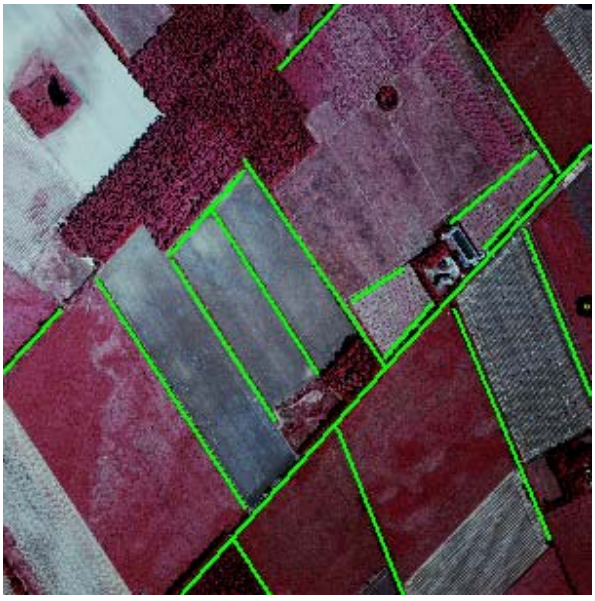

Fig. 11. Final results of extracted wind erosion obstacles

The extracted wind erosion obstacles are not only described by their direct appearance in geometry, but also a 2D elongated shadow region next to and in a known direction (e.g. northern direction at noon) according to their height information. First results of extracted wind erosion obstacles are quite satisfying (Figure 11). As can be seen, most wind erosion obstacles are extracted automatically, only one hedge (center of Figure 11) and a few short tree rows (bottom right of Figure 11) are missing. When compared with Figure 8, one can see that the line of the missed hedge is extracted and linked successfully. This line is grouped into the longer line because they are very close to each other and the DSM information is not enough precise.

5. CONCLUSIONS

An effective approach of extraction wind erosion obstacles to enhance the Digital Soil Science Map of Lower Saxony (Germany) by integrating GIS data, DSM and aerial imagery is presented. Prior knowledge from GIS and DSM is essential to facilitate the extraction of interested objects. The extracted wind erosion obstacles are not only described by their direct appearance in geometry, but also a 2D elongated shadow region next to and in a known direction according to their height information. All wind erosion obstacles are field boundaries or at least parallel with a short distance in between. This information can be integrated into the second process of extracting field boundaries. Furthermore, the extracted wind erosion obstacles can be used in many applications such as precision farming and soil preservation.

Extraction of wind erosion obstacles by integrating separately extracted field boundaries, orhthoimage (if available) and the data already used in this paper will be our work in the near future. An overall evaluation of separately extracted wind erosion obstacles and field boundaries to improve the completeness and correctness of the achieved results also need to be performed.

ACKNOWLEDGEMENT

The author would give many thanks to staffs of Institute of Photogrammetry and GeoInformation (IPI), University of Hannover, especially Prof. Konecny, Prof. Heipke and Dr. Jacobsen for giving the opportunity to do this interesting work while staying in IPI as a guest researcher.

This work is also supported by National Natural Science Foundation of China (NSFC) with project number 40301041.

REFERENCES

Baltsavias, E.P., 2002. Object Extraction and Revision by Image Analysis Using Existing Geospatial Data and Knowledge: State-of-The-Art and Steps Towards Operational Systems. IAPRS, Xi'an, Vol. XXXIV, Part 2, pp. 13-22.

Butenuth M., Heipke C., 2003. Modelling the Integration of Heterogeneous Vector Data and Aerial Imagery, Proceedings ISPRS Workshop on Challenges in Geospatial Analysis, Integration and Visualization II, Stuttgart, Sept. 8-9.

Campadelli P., Schettini R, Zuffi S., 2000 A system for the automatic selection of conspicuousness color sets for qualitative data display and visual interface design, Journal of Image and Graphics , Vol 5 (suppl), pp. 500-503.

De Moura M. L., Galvao L. S., 2003. Smoke effects on NDVI determination of savannah vegetation types. International Journal of Remote Sensing. Vol. 24, pp.4225 - 4231, 2003

Englisch, A., Heipke, C., 1998. Erfassung und Aktualisierung topographischer Geo-Daten mit Hilfe analoger und digitaler Luftbilder. PFG 3, pp. 133-149.

Heipke, C., Pakzad, K., Straub, B.-M., 2000. Image Analysis for GIS Data Acquisition. Photogrammetric Record, 16(96), pp. 963-985.

Lebrun V., Toussaint C., Pirard E, 2000. On the use of image analysis for quantitative monitoring of stone alteration. http://www.ulg.ac.be/mica/pdf files/Marble_Color_Alteration.pdf

Lyon J. G., Yuan D., Lunetta R., et al, 1998. A Change Detection Experiment Using Vegetation Indices. Photogrammetric Engineering and Remote Sensing, Vol. 64, pp. 143-150

Pierce P. E., Marcus R. T., 1994. Color and Appearance. Federation of Societies for Coatings Technology, Blue Bell.

Prince, S. D., 1991. Satellite Remote Sensing of Primary Production: Comparison of Results from Sahelian Grasslands 1981-1988, Internation Journal of Remote Sensing, Vol.12, pp. 1313-1330.

SEII EM-MI 2002. Theory perceive the color, introduction to graphic of computer. http://semmix.pl/color/default.htm.

Straub, B.-M., 2003. Automatic Extraction of Trees from Aerial Images and Surface Models, ISPRS Conference on Photogrammetric Image Analysis, September 17-19, Munich, Germany

Zhang Y. J., Zhang Z. X., Zhang J. Q., 2003. 3D Reconstruction of Industrial Sheetmetal Parts with Hybrid Point-line Photogrammetry. SPIE Third International Symposium on Multispectral Image Processing and Pattern Recognition, 20-22 October 2003, Beijing, China